Slickenside as a record of weak shock metamorphism in the surface layer of asteroid Ryugu

Masaaki Miyahara[1*], Takaaki Noguchi[2], Toru Matsumoto[2,3], Naotaka Tomioka[4], Akira Miyake[2], Yohei Igami[2], Yusuke Seto[5], Mitsutaka Haruta[6], Hikaru Saito[7,8], Satoshi Hata[9,10], Hope A. Ishii[11], John P. Bradley[11], Kenta K. Ohtaki[11], Elena Dobrică[11], Hugues Leroux[12], Corentin Le Guillou[12], Damien Jacob[12], Francisco de la Peña[12], Sylvain Laforet[12], Bahaeeddine Mouloud[12], Maya Marinova[13], Falko Langenhorst[14], Dennis Harries[15], Pierre Beck[16], Thi H. V. Phan[16], Rolando Rebois[16], Neyda M. Abreu[17], Jennifer Gray[18], Thomas Zega[19], Pierre-M. Zanetta[19], Michelle S. Thompson[20], Rhonda Stroud[21], Kate Burgess[22], Brittany A. Cymes[23], John C. Bridges[24], Leon Hicks[24,25], Martin R. Lee[26], Luke Daly[26,27,28], Phil A. Bland[29], Michael E. Zolensky[30], David R. Frank[11], James Martinez[31], Akira Tsuchiyama[32,33,34], Masahiro Yasutake[35], Junya Matsuno[32], Shota Okumura[2], Itaru Mitsukawa[2], Kentaro Uesugi[35], Masayuki Uesugi[35], Akihisa Takeuchi[35], Mingqi Sun[33,34,36], Satomi Enju[37], Aki Takigawa[38], Tatsuhiro Michikami[39], Tomoki Nakamura[40], Megumi Matsumoto[40], Yusuke Nakauchi[41], Masanao Abe[41,42], Satoru Nakazawa[41], Tatsuaki Okada[41,42], Takanao Saiki[41], Satoshi Tanaka[41,42], Fuyuto Terui[43], Makoto Yoshikawa[41,42], Akiko Miyazaki[41], Aiko Nakato[41], Masahiro Nishimura[41], Tomohiro Usui[41], Toru Yada[41], Hisayoshi Yurimoto[44], Kazuhide Nagashima[11], Noriyuki Kawasaki[44], Naoya Sakamotoa[45], Ryuji Okazaki[46], Hikaru Yabuta[9], Hiroshi Naraoka[46], Kanako Sakamoto[41], Shogo Tachibana[47], Sei-ichiro Watanabe[48], Yuichi Tsuda[41]

[1]Graduate School of Advanced Science and Engineering, Hiroshima University, 1-3-1 Kagamiyama, Higashi-Hiroshima, Hiroshima, 739-8526, Japan.
[2]Division of Earth and Planetary Sciences, Kyoto University, Kitashirakawaoiwake-cho, Sakyo-ku, Kyoto 606-8502, Japan.
[3]The Hakubi Center for Advanced Research, Kyoto University, Kitashirakawaoiwake-cho, Sakyo-ku, Kyoto 606-8502, Japan.
[4]Kochi Institute for Core Sample Research, X-star, JAMSTEC, 200 Monobe Otsu, Nankoku, Kochi 783-8502, Japan.
[5]Department of Geosciences, Osaka Metropolitan University, Sugimoto 3-3-138, Sumiyoshi-ku, Osaka 558-8585, Japan.
[6]Institute for Chemical Research, Kyoto University, Gokasho, Uji, Kyoto 611-0011, Japan.
[7]Institute for Materials Chemistry and Engineering, Kyushu University, Fukuoka 816-8580, Japan.
[8]Pan-Omics Data-Driven Research Innovation Center, Kyushu University, Fukuoka 816-8580, Japan.
[9]Interdisciplinary Graduate School of Engineering Sciences, Kyushu University, Fukuoka 816-8580, Japan.
[10]The Ultramicroscopy Research Center, Kyushu University, Fukuoka 819-0395, Japan.
[11]Hawai'i Institute of Geophysics and Planetology, The University of Hawai'i at Mānoa, 1680 East-West Road, POST Building, Room 602, Honolulu, HI 96822, USA.
[12]Université de Lille, CNRS, INRAE, Centrale Lille, UMR 8207-UMET-Unité Matériaux et Transformations, F-59000 Lille, France.
[13]Université de Lille, CNRS, INRAE, Centrale Lille, Université Artois, FR 2638-IMEC-Institut Michel-Eugène Chevreul, F-59000 Lille, France.
[14]Institut für Geowissenschaften, Friedrich-Schiller-Universität Jena, Carl-Zeiss-

Promenade 10, 07745 Jena, Germany.
[15]European Space Resources Innovation Centre, Luxembourg Institute of Science and Technology, 41 rue du Brill, 4422 Belvaux, Luxembourg.
[16]Université Grenoble Alpes, CNRS, IPAG, 38000 Grenoble, France.
[17]NASA Langley Research Center, Hampton, VA 23681-2199, USA.
[18]Materials Characterization Lab, The Pennsylvania State University Materials Research Institute, Millennium Science Complex, Pollock Road, University Park, PA16802, USA.
[19]Lunar and Planetary Laboratory, Department of Planetary Sciences, The University of Arizona, 1629 E. University Blvd., Tucson AZ 85721-0092, USA.
[20]Department of Earth, Atmospheric and Planetary Sciences, Purdue University, 550 Stadium Mall Drive, West Lafayette, IN 47907-2051, USA.
[21]Buseck Center for Meteorite Studies, Arizona State University, 781 E Terrace Road, Tempe, AZ 85281, USA.
[22]Materials Science and Technology Division, U.S. Naval Research Laboratory, Washington, DC 20375, USA.
[23]NRC Postdoctoral Research Associate, U.S. Naval Research Laboratory, Washington, DC 20375, USA.
[24]Space Park Leicester, University of Leicester, 92 Corporation Road, Leicester, LE4 5SP, UK.
[25]School of Geology, Geography and the Environment, The University of Leicester, University Road, Leicester, LE1 7RH, UK.
[26]School of Geographical and Earth Sciences, The University of Glasgow, Molema Building, Lilybank Gardens, Glasgow G12 8QQ, UK.
[27]Australian Centre for Microscopy and Microanalysis, The University of Sydney, Sydney, New South Wales, Australia.
[28]Department of Materials, The University of Oxford, Parks Road, Oxford, OX1 3PH, UK.
[29]School of Earth and Planetary Sciences, Curtin University, GPO Box U1987, Perth, Western Australia 6845, Australia.
[30]ARES, NASA Johnson Space Center, 2101 NASA Parkway, Houston, Texas 77058, USA
[31]Jacobs Engineering, 1999 Bryan Street, Suite 1200, Dallas, Texas 75201, USA.
[32]Research Organization of Science and Technology, Ritsumeikan University, 1-1-1 Nojihigashi, Kusatsu, Shiga 525-8577, Japan.
[33]CAS Key Laboratory of Mineralogy and Metallogeny, Guangdong Provincial Key Laboratory of Mineral Physics and Materials, Guangzhou Institute of Geochemistry, Chinese Academy of Sciences (CAS), Guangzhou 510640, China.
[34]CAS Center for Excellence in Deep Earth Science, Guangzhou 510640, China.
[35]Japan Synchrotron Radiation Research Institute, 1-1-1 Kouto, Sayo-cho, Sayo-gun, Hyogo 679-5198, Japan.
[36]University of Chinese Academy of Sciences, Beijing 100049, China.
[37]Department of Mathematics, Physics, and Earth Science, Ehime University, 2-5 Bunkyo-cho, Matsuyama, Ehime 790-8577, Japan.
[38]Department of Earth and Planetary Science, The University of Tokyo, 7-3-1 Hongo, Bunkyo-ku, Tokyo 113-0033, Japan.
[39]Faculty of Engineering, Kindai University, Hiroshima Campus, 1 Takaya Umenobe, Higashi-Hiroshima, Hiroshima 739-2116, Japan.

[40]Department of Earth Science, Tohoku University, 6-3 Aoba, Aramaki, Aoba-ku, Sendai 980-8578, Japan.
[41]Institute of Space and Astronautical Science, Japan Aerospace Exploration Agency, 3-1-1 Yoshinodai, Chuo-ku, Sagamihara, Kanagawa 252-5210, Japan.
[42]The Graduate University for Advanced Studies, SOKENDAI, Hayama 240-0193, Japan.
[43]Department of Mechanical Engineering, Kanagawa Institute of Technology, Atsugi 243-0292, Japan.
[44]Department of Earth and Planetary Sciences, Hokkaido University, Kita-10 Nishi-8, Kita-ku, Sapporo 060-0810, Japan.
[45]Creative Research Institution Sousei, Hokkaido University, Kita-21, Nishi-10, Kita-ku, Sapporo 001-0021, Japan.
[46]Department of Earth and Planetary Sciences, Kyushu University, 744 Motooka, Nishi-ku, Fukuoka 819-0395, Japan.
[47]UTokyo Organization for Planetary and Space Science, The University of Tokyo, 7-3-1 Hongo, Bunkyo-ku, Tokyo 113-0033, Japan.
[48]Department of Earth and Environmental Sciences, Nagoya University, Furo-cho, Chikusa-ku, Nagoya 464−8601, Japan.

Corresponding author: Masaaki Miyahara (miyahara@hiroshima-u.ac.jp)

Abstract

The surface morphology of regolith grains from the C-type asteroid Ryugu was studied in search of evidence of impact events on the asteroid. Scanning electron microscopy revealed that ~8% of C0105-042 Ryugu grains have a smooth surface on one side of the grains. One of these grains has striated linear grooves (striations) on its smooth surface. Transmission electron microscopy of the grain showed that a porous fine-grained Mg-Fe phyllosilicate assemblage, which is the main component of Ryugu grains, is compacted as it approaches the smooth surface. The smooth surface with striations closely resembles a slickenside, a characteristic texture found in terrestrial fault rocks formed by shear deformation. There is no evidence of melting/decomposition in the Mg-Fe phyllosilicates near the smooth surface, indicating that the shear heating temperature is less than ~1100 K. Assuming that the average length of the striations corresponds to the minimum displacement of the micro-fault, the shock pressure recorded in the C0105-042 Ryugu grains is estimated to be < ~4.5 GPa by a fault mechanics calculation. The shock pressures of C0105-042, together with those of C0014 (~2 GPa) and C0055 (>~3.9 GPa) in previous studies suggest that the impact velocities recorded in these grains are < ~0.89–1.63 km/s. Based on the impact velocities, these grains may record an impact event that occurred when asteroid Ryugu was in the main belt orbit.

Introduction

A celestial collision is one of the fundamental phenomena in the evolution of a body in the solar system. The rocks and minerals of a body are physically and chemically affected by the high-pressure and high-temperature conditions induced by the collision of another body. Evidence of shock metamorphism is recorded in meteorites, lunar rocks from the Apollo missions, and Itokawa grains from the Hayabusa mission, which have been studied collectively for several decades to understand the evolution of bodies in the solar system (e.g., El Goresy et al., 2013; Kaneko et al., 2015; Kayama et al., 2012; Kimura et al., 2017; Miyahara et al., 2021; Miyahara et al., 2020; Ohtani et al., 2004; Stöffler et al., 2018; Tomeoka et al., 2001; Zolensky et al., 2022a).

The Hayabusa2 spacecraft shows that the C-type asteroid Ryugu has large surface boulders, suggesting a rubble-pile structure (Watanabe et al., 2019), and the boulders have layered structures (Sugita et al., 2019; Tachibana et al., 2022). The boulders having layered structures can be regarded as subparallel cracks, which is one of the notable features associated with strong shock metamorphism (Nakamura et al., 2000; Tomeoka et al., 1999). It is clear from the external features obtained by the spacecraft that the asteroid Ryugu has experienced repeated collisions and destruction.

The degree of shock metamorphism in the bulk rock of a meteorite is evaluated by microscopic comparisons with recovered samples from shock experiments of meteorites with the same characteristics as the meteorite. The cosmochemical and mineralogical characters of Ryugu grains are most similar to CI chondrites (Ito et al., 2022; Nakamura et al., 2022; Nakamura et al., 2023; Yokoyama et al., 2023). However, a shock and recovery experiment with a CI chondrite has not been performed because of the rarity of the sample and the difficulty of sample recovery due to the high volatile content causing explosive dispersal by post-shock heating.

The degree of shock-induced deformation depends on the volume ratio of the matrix to the chondrule and the porosity of the matrix (Kieffer, 1971; Sharp and DeCarli, 2006). Among the carbonaceous chondrites, CM chondrites have the second highest ratio of matrix to chondrule after CI chondrites (Weisberg et al., 2006). Therefore, CM chondrites can be used as simulants for CI chondrites to evaluate shock metamorphism. Based on the shock and recovery experiments using the Murchison CM2 chondrite, deformation and melting of a matrix occur with increasing shock pressure, as well as an increase in the aspect ratio of the chondrules and the density of subparallel cracks (Tomeoka et al., 1999).

Subparallel cracks and micro-faults that are considered to correspond to shock stage S1 (< 4–5 GPa) are discovered in C0014 and C0055 Ryugu grains (Kikuiri et al.,

2022; Nakamura et al., 2023; Tomioka et al., 2023). However, in the case of low shock stages of S1–S2 (< 10 GPa), the diagnostic shock features, which can be used as an indicator of the specific shock pressure, are poorly understood (Stöffler et al., 2018). Ryugu grains have undergone only weak shock metamorphism, and there is a lack of statistical data on the shock pressures of the respective Ryugu grains. Therefore, the determination of representative pressure experienced by the Ryugu grains, is still difficult. Meteoroid impacts have vitrified and/or melted some Ryugu grains to ~1 μm depth below the surface (Noguchi et al., 2023). In other words, shock metamorphism is recorded not only throughout the grain, but also on the surface of Ryugu grains as space weathering textures. In the present study, we examine the surface morphology and subsurface microtextures of C0105 Ryugu grains and report new evidence of weak impact that allows us to estimate the shock pressure of an impact that occurred on asteroid Ryugu.

Samples and experimental methods

Ryugu grains, averaging ~100 μm in diameter, from chamber C (C0105 aggregate grains collected from the second touchdown) were attached to a gold (Au) plate (sample plate number: C0105-042) with small amounts of epoxy adhesive in an N_2-filled glove box for surface morphology observation. The surface morphology of the grains without any coating was observed using JEOL JSM-7100F and Hitachi S-5200 field emission gun scanning electron microscopes (FEG-SEM) at the faculty of engineering, Tohoku University and Natural Science Center for Basic Research and Development (NBARD), Hiroshima University, respectively. Observations were made by secondary electron (SE) imaging (at a low accelerating voltage of 3.0–5.0 kV) to study the surface morphology. The chemical composition of Ryugu grains was measured using a JEOL energy dispersive spectrometer (EDS) attached to a JEOL JSM-7100F SEM.

Some parts in the grains were excavated and processed into ultrathin films using a Hitachi SMI4050 focused ion beam (FIB) system at the Kochi Institute for Core Sample Research, Japan Agency for Marine-Earth Science and Technology (JAMSTEC), after coating with osmium and carbon to ensure the electron conductivity of the grain surface. First, a tungsten protection layer was deposited on a target portion using a weak gallium (Ga) ion beam (30 kV, 40 pA) in the FIB to avoid ion irradiation damage. The portions were then thinned to a thickness of ~1–2 μm and cut out using a Ga-ion beam at an accelerating voltage of 30 kV, and the thin sections were mounted on Cu grids using a micromanipulator equipped with the FIB. Phyllosilicate minerals, which are abundant in carbonaceous chondrites, are sensitive to Ga ion beams. Therefore, the thin sections were ultrathinned to a thickness of ~100 nm using a very weak Ga ion beam (30 kV, 40 pA).

Finally, the ultrathin films were tilted 15 degrees and cleaned with a low voltage Ga ion beam (5 kV, 40 pA) to remove the damaged layer on the surface of the ultrathin films. The ultrathin films were examined by a JEOL JEM-2100F field emission gun transmission electron microscope (FEG-TEM) operating at 200 kV equipped with a JEOL EDS at the Faculty of Engineering, Tohoku Univ. The TEM mode was used for conventional TEM observation and selected area electron diffraction (SAED) pattern analysis. The chemical compositions were measured by EDS under scanning TEM (STEM) mode.

Results

The surface morphology of more than twenty-four grains (C0105-042_No. 1–24) was observed by SE imaging. When the grains were placed on the Au plate, some of them broke, exposing new surfaces. Most grains have a bumpy or rough surface, and some grains show signs of space weathering, having once been melted or vitrified by meteoroid impacts or cosmic radiation (Noguchi et al., 2023). On the other hand, two grains (C0105-042_No. 22, 24) have a smooth surface on one side of the grain (Fig. 1a). In view of the aspect and chemical composition of the grains, the smooth surface is not a specific surface of a single crystal mineral (Fig. 1b). The surface was also observed by secondary ion imaging in FIB (Fig. 1c) before microfabrication. The images showed striated linear grooves (striations): average length: 5.58 μm, n = 4 on the smooth surface (Fig. 1d).

An ultrathin TEM foil was prepared by FIB from the smooth surface with a striation from the C0105-042_No. 24 grain to observe its cross section by TEM (Fig. 1c). High-angle annular dark-field (HAADF) and X-ray elemental mapping images of the TEM foil are shown in Figure 2a–e. The TEM foil consists only of matrix minerals: fibrous Mg-Fe phyllosilicate (saponite and serpentine) assemblages (Fig. 2f) embedding small amounts of fine-grained iron sulfides and iron oxide grains. The bright field (BF)-TEM image of the matrix away from the smooth surface shows that the fibrous Mg-Fe phyllosilicate minerals are loosely aggregated and there are many interstices between the fibrous Mg-Fe phyllosilicate aggregates (Fig. 3a). Some interstices are filled with carbonaceous materials (Fig. 2b). These morphological and mineralogical characteristics observed in the C0105-042_No. 24 grain are similar to the matrices of other Ryugu grains described in previous studies (Nakamura et al., 2022; Nakamura et al., 2023; Noguchi et al., 2023).

In contrast, the fibrous Mg-Fe phyllosilicate assemblages near the smooth surface are densely aggregated with fewer interstitial spaces, making it difficult to distinguish individual Mg-Fe phyllosilicate assemblages (Fig. 3b). Lattice fringes corresponding to

Mg-Fe phyllosilicates become obscured approaching smooth surface, indicating vitrification or dehydration. The region from the smooth surface to about 200 nm is particularly dense, where the Mg-Fe phyllosilicate packages are nearly parallel to the smooth surface in some areas (Fig. 3b). The exact values of the individual lattice spacings could not be determined because the Mg-Fe phyllosilicates were compressed and overlapped in the TEM foil. The mosaic BF-TEM image shows that the degree of compaction in the Mg-Fe phyllosilicate assemblages increases toward the smooth surface (from less compacted to highly compacted Mg-Fe phyllosilicates in Fig. 4).

At high temperatures and pressures, Mg-Fe phyllosilicates decompose into several minerals (e.g., forsterite and enstatite) and experience dihydroxylation (e.g., Akai, 1992). At higher temperatures and pressures, melting of Mg-Fe phyllosilicates occurs. However, TEM observations showed that neither melting nor decomposition of Mg-Fe phyllosilicates was observed, even just below the smooth surface. In addition, no high-pressure minerals (e.g., zolenskyite) (Tomioka et al., 2023) were identified in the TEM foil.

Discussion

About 8% of C0105-042 Ryugu grains have a smooth surface on a portion of the grain. Some Ryugu grains have such smooth surfaces, which is due to space weathering. The space weathering layers have bubble and blister microtextures (Noguchi et al., 2023). However, the smooth surfaces found in our study are quite different from the space weathering layers, but have striations and traces of compression (Figs. 1–4). There are three possible scenarios to explain the formation of the smooth surface on C0105-042_No. 24 Ryugu grain: i) weathering or alteration, ii) abrasion between grains, and iii) faulting within a grain.

The scenario (i) will be discussed first. Some carbonaceous chondrites have veinlets filled with terrestrial weathering and/or alteration products such as carbonate, calcium sulfate, and iron hydroxide (Gounelle and Zolensky, 2001; Richardson, 1978). These veinlets may appear to have smooth surfaces when peeled along the vein. However, elemental mapping images show that carbonate, calcium sulfate, or iron hydroxide minerals do not preferentially occur along the smooth surface of the C0105-042_No. 24 Ryugu grain (Fig. 2b–e), indicating that the smooth surface is not a terrestrial weathering or alteration veinlet.

Then we will discuss the scenario (ii) : abrasion between grains. The surface of asteroid Ryugu is covered with millimeter-sized grains and centimeter- to meter-sized boulders (Michikami et al., 2019; Ogawa et al., 2022; Tachibana et al., 2022). When an

impactor strikes asteroid Ryugu, compaction due to shock wave propagation causes abrasion between randomly rolling grains/boulders, resulting in the formation of a polished surface. However, this scenario is probably unlikely due to the high macro-porosity of asteroid Ryugu (~16%) estimated from the boulder size-frequency distribution (Grott et al., 2020). Numerical simulations show that Amonton's law, which says that the frictional force does not depend on the apparent contact area and is proportional to the loading force (Bowden and Tabor, 2001), breaks down for an elastic object (Otsuki and Matsukawa, 2013). Asteroid Ryugu is formed by the loose accumulation of boulders by gravity. If loosely aggregated rocks behave elastically below the Hugoniot elastic limit (HEL), the internal friction coefficient of the bulk grain/boulder system may be reduced. The amount of heat generated by friction depends on the friction coefficient, normal stress, and momentum. When the normal stress and momentum are constant, the smaller the friction coefficient, the smaller the amount of heat generated by friction. Therefore, the scenario (ii) would be valid only if the shock pressure exceeds the HEL of the loosely aggregated rocks, although a quantitative evaluation is currently difficult.

The scenario (iii), shock-induced faulting in a grain as the formation mechanism of the smooth surface, is the most plausible because the smooth surface of the C0105-042_No. 24 Ryugu grain is similar to a slickenside. A slickenside is a well-polished surface with a thickness of the order of 100 μm, and the surface is composed of fine grains with a diameter of 0.01–1 μm, formed on a shear plane in a terrestrial fault rock and shatter cones around impact craters (Baratoux and Reimold, 2016; Doblas et al., 1997; Kirkpatrick et al., 2013; Power and Tullis, 1989; Sagy and Brodsky, 2009). A striation is one of the characteristic morphological features of a slickenside, which is present on the smooth surface of the C0105-042_No. 24 Ryugu grain (Fig. 1d). The fibrous Mg-Fe phyllosilicate assemblage near the smooth surface is the most compacted (Figs. 3b, 4), supporting our interpretation that the slickenside-like texture was formed by shock compression. The formation processes of slickenside and shock-melt veins in meteorites are alike (Gillet and El Goresy, 2013), although a melting texture is not observed near the smooth surface of the C0105-042_No. 24 Ryugu grain (Fig. 3b). When a shock-induced faulting occurs in the Ryugu grain, a smooth surface is then formed along the fault plane mainly due to the plastic deformation of Mg-Fe phyllosilicates, but melting does not occur along the fault plane, so it is not strongly adhered. Therefore, Ryugu grains containing such faults are easily detached along the fault planes, resulting in the exposure of smooth surfaces.

Based on the shock and recovery experiments using Murchison CM2, the remarkable features of shock metamorphism such as dense fractures and flattened

chondrules appear above ~20 GPa (Tomeoka et al., 1999). However, these features related to shock metamorphism are not found in the C0105-042 Ryugu grains. Alternatively, we can estimate the shock pressure recorded in the smooth-surfaced Ryugu grain by assuming that the faulting by shock is analogous to that causing earthquakes on Earth. A micro-fault-like vein, recognizable by the presence of an elongated framboidal magnetite, is found in C0014 Ryugu grain (Tomioka et al., 2023). Tomioka et al. (2023) estimated the approximated mean stress: P_m ($[s_1 + s_3]/2$: $s_1 > s_2 \approx s_3$) applied to the micro-fault using the following equation (Jaeger et al., 2009; Kanamori et al., 1998):

$$P_m = \Delta T C d \rho \, (1 + \mu^2)^{0.5} / \mu D$$

where ΔT, C, d, ρ, μ, and D are temperature increase, heat capacity of bulk rock, fault thickness, density of bulk rock, friction coefficient, and displacement along the fault, respectively. We estimate the stress applied to form the smooth surface by using this equation. ΔT corresponds to localized temperature increase at the smooth surface. According to serpentine heating experiments, dehydration occurs up to 473 K, followed by dehydroxylation in the 873–1073 K range, which is accompanied by decomposition of the crystal structure and a change to the amorphous state (Akai, 1992; Ball and Taylor, 1963; Brindley and Hayami, 1963; Cattaneo et al., 2003; Weber and Greer, 1965). Finally, forsterite and enstatite crystallize from the amorphous material above 1073 K. Saponite decomposes to enstatite above 1100 K after dehydration around 473 K (Akai, 1992). Neither the melting nor decomposition of Mg-Fe phyllosilicates (saponite and serpentine) are found near the smooth surface of C0105-042_No. 24 Ryugu grain (Fig. 3b). Considering the difference between the decomposition temperature of saponite and serpentine (~1100 K) and the lowest temperature of the current Ryugu surface is ~300 K (Sugita et al., 2019), the maximum ΔT is assumed to be ~800 K. C, ρ, and μ values used in this calculation are the same as those used in the calculations in Tomioka et al. (2023). The fibrous Mg-Fe phyllosilicate assemblage is strongly compacted from the smooth surface to a depth of ~1 μm (Fig. 4). Assuming that the C0105-042_No. 24 Ryugu grain was detached at half the thickness of the compression layer, the original thickness d of the fault zone is 2 μm. A striation appears on the smooth surface (Fig. 2d), consisting of scratches along a displacement direction. Hence, the average length of the striations (5.58 μm, $n = 4$) could be regarded as the minimum D value. By adopting these parameters into the equation, the peak shock pressure is estimated to be less than ~4.5 GPa (Fig. 5). The C0105-042 Ryugu grains, which were collected near a crater formed by the small carry-on impactor (SCI) (Arakawa et al., 2020), may have been affected by SCI impact event.

However, this is unlikely because shock physics calculations estimate that < 0.003 vol% of the grains ejected from the crater experienced >2 GPa from the SCI impact (Tomioka et al., 2023).

Preliminary analysis of more than 39 Ryugu grains (including C0014, C0055, and C0105-042) indicates that most of the Ryugu grains do not show any significant evidence of strong shock metamorphism (Ito et al., 2022; Nakamura et al., 2022; Nakamura et al., 2023; this study). The estimated shock pressure of the C0014 and C0105-042 Ryugu grains are ~2 GPa (Tomioka et al., 2023) and < ~4.5 GPa (this study), respectively. Only C0055 grain shows evidence of uniaxial compression and sets of subparallel fractures, which is suggestive of a shock pressure more than ~3.9 GPa following the shock and recovery experiments of Murchison CM2 (Kikuiri et al., 2022; Nakamura et al., 2023; Tomeoka et al., 1999). The shock classification of the Ryugu grains examined at a first stage of analysis is smaller than S3 (< 10 GPa). There are several similarities in constituent minerals and physical characteristics between CM and CI chondrite: i) abundant hydrous phyllosilicates, ii) low density, and iii) low chondrule/matrix ratio (Consolmagno et al., 2008; Flynn et al., 1999; Weisberg et al., 2006). Although a systematic study of a shock classification of CI chondrites has not been made, the tendency of the shock classification of Ryugu grains is similar to that of CM chondrites (Scott et al., 1992). A trace amount of possible shock-induced melts is found only in the Orgueil CI chondrite (Zolensky et al., 2022b). It is obvious that the shock metamorphism degree of CI chondrites is weak compared to ordinary and enstatite chondrites (e.g., Bischoff et al., 2018; Miyahara et al., 2020; Scott et al., 1992; Tomioka and Miyahara, 2017). A parent-body of CI chondrites is fragile because i) it is made with a porous H_2O-bearing building block: hydrous Mg-Fe phyllosilicate assemblage, ii) very low tensile strength (0.7–2.8 MPa for the Ivuna and Orgueil CI1 chondrites) (Tsuchiyama et al., 2008), and iii) very high porocity (~34.9% for the Orgueil CI1 chondrite)(Macke et al., 2011). Hence, the body would be easily demolished even by weak shock metamorphism (Scott et al., 1992; Tomeoka et al., 2003).

Asteroid Ryugu has experienced repeated collisions (Watanabe et al., 2019). Its surface rocks are breccias (Sugita et al., 2019; Tachibana et al., 2022) and may have recorded several different impact events. It is difficult to clarify each impact event that occurred on the asteroid Ryugu. Nevertheless, it would be possible to discuss the average impact events experienced by asteroid Ryugu, taking into account the shock metamorphism estimated for other grains. Based on the estimated shock pressure of C0014, C0055, and C0105-042 Ryugu grains, the impact velocity of a meteoroid striking

asteroid Ryugu could be roughly calculated. The impact pressure (P) on the surface of asteroid Ryugu can be expressed according to the Rankine-Hugoniot relations as follows:

$$P = \rho_0 V_p U \qquad \text{eq. (1)}$$

where ρ_0, V_p, and U are the density before impact, particle velocity, and shock wave velocity, respectively. We assumed the initial average bulk density of Ryugu grains: ρ_0 = 1.79 kg/m$_3$ (Nakamura et al., 2023). The relationship between the shock wave velocity (U) and the particle velocity (V_p) can be expressed by the following equation:

$$U = c_0 + s V_p \qquad \text{eq (2)}$$

where c_0 and s are the bulk sound velocity and the dimensionless parameter depending on the material, respectively. Assuming that the meteoroid hitting the asteroid Ryugu and Ryugu are of the same material, the particle velocity (V_p) can be expressed by the following equation:

$$V_p \approx V_i/2 \qquad \text{eq (3)}$$

where V_i is the impact velocity. The Hugoniot equation of state for CI chondrites has not yet been determined. Instead, we used the Hugoniot data for Murchison CM2 as a simulant for CI chondrites and calculated the shock pressures assuming c_0 = 1.87 km/s, s = 1.48 (Anderson and Ahrens, 1998). For shock pressures (P) of 2 GPa (C0014) and 4.5 GPa (C0105-042), the estimated impact velocities are ~0.89 km/s and ~1.63 km/s, respectively.

Asteroid Ryugu was decoupled from the main belt orbit and placed in a near-Earth orbit about 5 Myr ago (Okazaki et al., 2023). The B-type asteroid Bennu is also a near-Earth asteroid (NEAs) made of hydrated materials (Hamilton et al., 2019; Lauretta et al., 2022). The impact velocities distribution of meteoroids derived from cometary sources striking asteroid Bennu is estimated using NASA's Meteoroid Engineering Model, and the peak impact velocities are over 20 km/s (Bottke et al., 2020). The impact velocity is much faster than the average impact velocity (~4.4 km/s) of meteoroids derived from asteroidal sources striking an asteroid in the main belt (Bottke et al., 1994). Although the likelihood of an impact by a large cometary source meteoroid is probably very small, asteroid Ryugu probably also experienced such a high-volocity impact while in near-Earth orbit. Such a high velosity impact causes strong shock heating effects as demonstrated in experimentally shocked Murchison CM2 chondrite; the matrix is totally melted at 49 GPa (Tomeoka et al., 2003; Tomeoka et al., 1999; Tomioka et al., 2007). This shock pressure corresponds to the impact velosity of 8.98 km/s from the Hugoniot of Murchison CM2 chondrite (Anderson et al. 1998). Thus, Ryugu materials would be shock-melted, if they have experienced similar impact events like asteroid Bennu in the NEA orbit.

In contrast, the impact velocities recorded for the whole Ryugu grains in C0014, C0055, and C0105-042 are much slower (< ~0.89–1.63 km/s). Based on data from the Rosetta spacecraft, the dust size distribution of comet 67P/Churyumov-Gerasimenko ranges from 0.1 to 1000 μm (Rinaldi et al., 2017). The impact velocities of cometary particles striking NEAs is high. However, the mass of each particle is too small to provide enough energy to metamorphose entire Ryugu grains, and it only produces a space-weathering layer instead. In fact, thin molten layers on the surface of some Ryugu grains (e.g., A0104 and C0105 Ryugu grains) (Noguchi et al., 2023) are evidence for ultra-high velocity micro-meteoroid impacts on asteroid Ryugu. The impact velocities recorded in Ryugu grains C0014, C0055, and C0105-042 are rather close to the average impact velocity between asteroids in the main belt. These impact records were probably made when the asteroid Ryugu was orbiting in the main belt.

The smooth surface (slickenside) found in C0105-042 Ryugu grains is too thin to survive atmospheric entry heating or terrestrial weathering. We could say that surface morphology analysis of returned samples is important not only from the perspective of space weathering, but also in terms of shock metamorphism because a slickenside as a shock deformation texture has not been found in meteorites and cosmic dust collected on Earth. Knowledge of the impact metamorphism of C- and B-type asteroids is still poor. The OSIRIS-REx spacecraft has recovered samples from the surface of B-type asteroid Bennu using the touch-and-go sample acquisition mechanism (Bierhaus et al., 2018; Lauretta et al., 2022). Therefore, it is expected that further information about the impacts that occurred on the surface of B-type asteroids can be obtained by analyzing not only the interior of the recovered particles, but also the surface of the particles.

Acknowledgments

Two anonymous reviewers are acknowledged for their helpful comments that improved an earlier version of this manuscript. This study was supported by a Grant-in-aid for Scientific Research, Nos. 18H01269 from MEXT to M.M. We thank Drs. T. Miyazaki (the faculty of engineering, Tohoku University) and M. Maeda (NBARD, Hiroshima University) for their assistance in the use of SEM and TEM instruments.

Conflict of Interest – The authors declare that there is no conflict of interest.

Data Availability – The data that support the findings of this study are available from the corresponding author upon reasonable request.

Figure legends

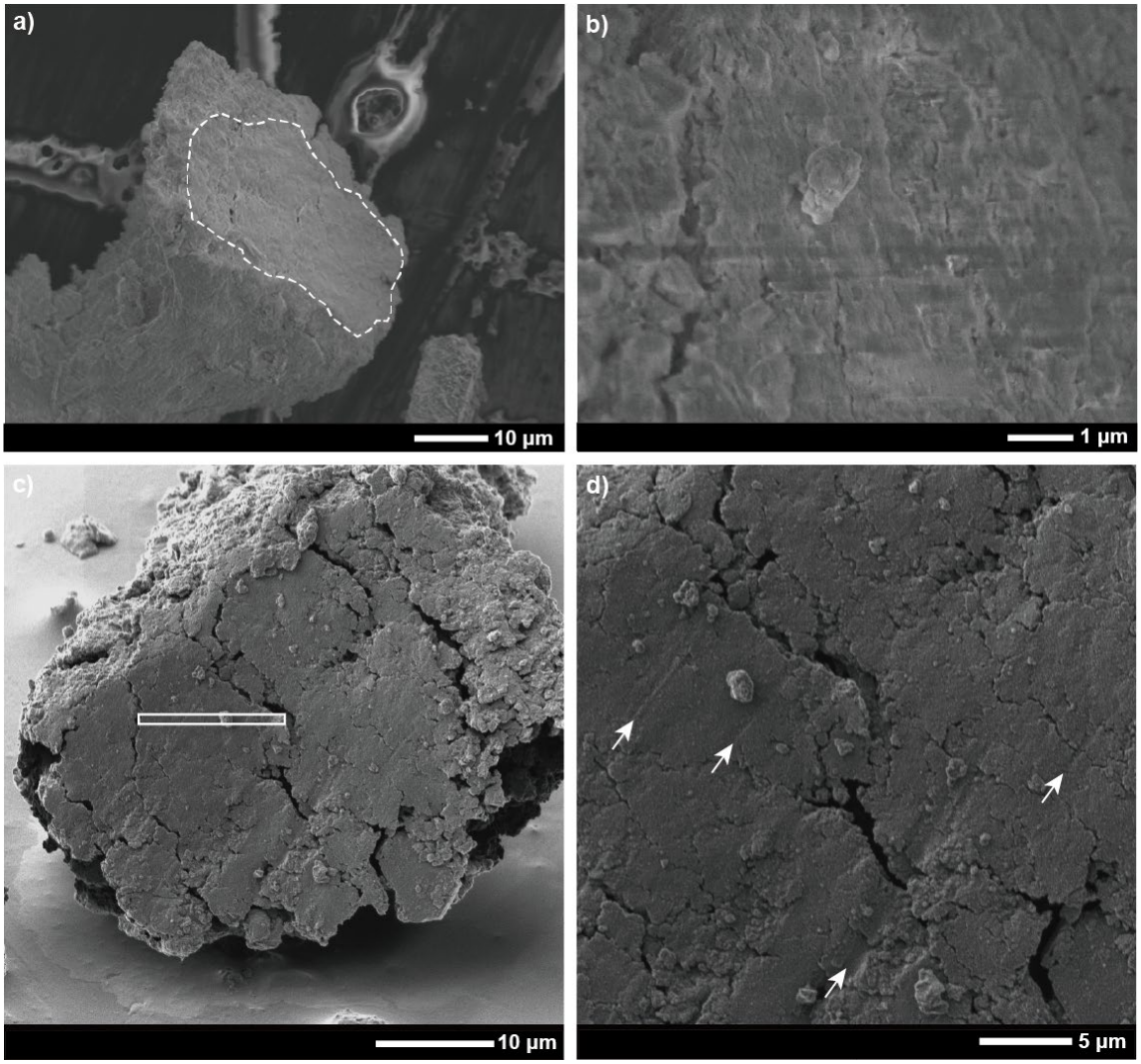

Figure 1. A grain with a smooth surface (C0105-042_No. 24). a) Secondary electron (SE) image of a grain with a smooth surface (dashed line), b) A high magnification SE image of the smooth surface. Horizontal parallel stripes are artifacts due to electron charge-up. c) Secondary ion (SI) image of a grain with a smooth surface (taken from the front of a smooth surface). The TEM foil excavated by the FIB is indicated by a white box. d) A high magnification SI image of the smooth surface. A striation is indicated by a white arrow.

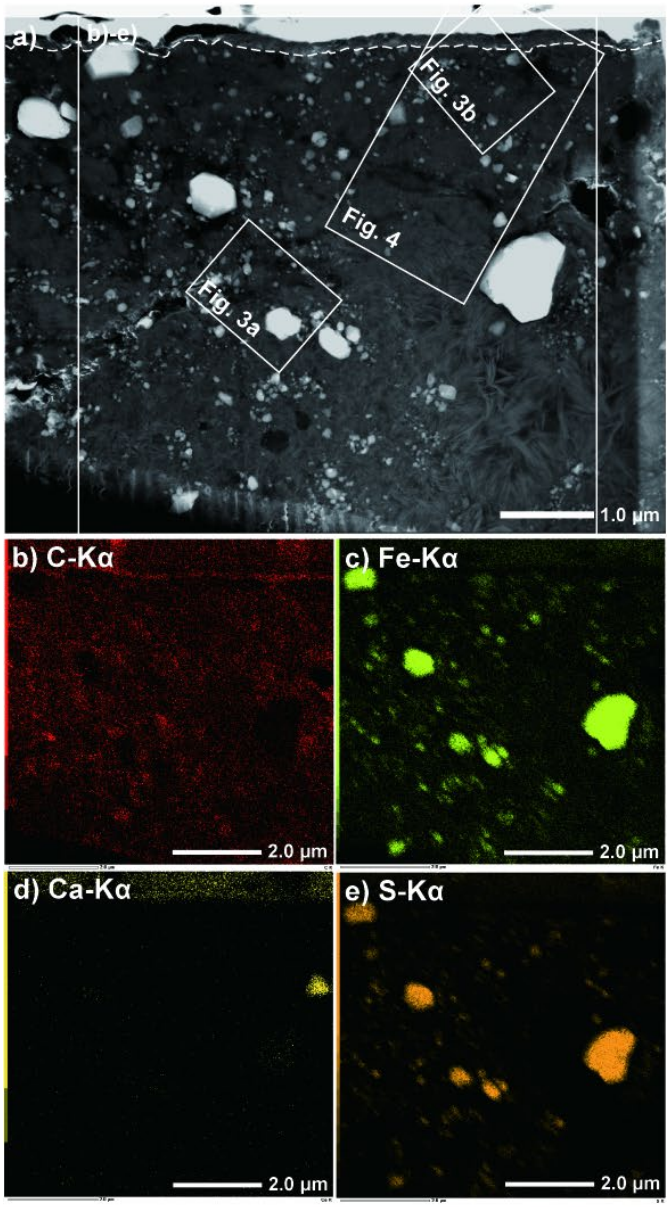
a)
b)-e)
Fig. 3b
Fig. 4
Fig. 3a
1.0 µm
b) C-Kα
2.0 µm
c) Fe-Kα
2.0 µm
d) Ca-Kα
2.0 µm
e) S-Kα
2.0 µm

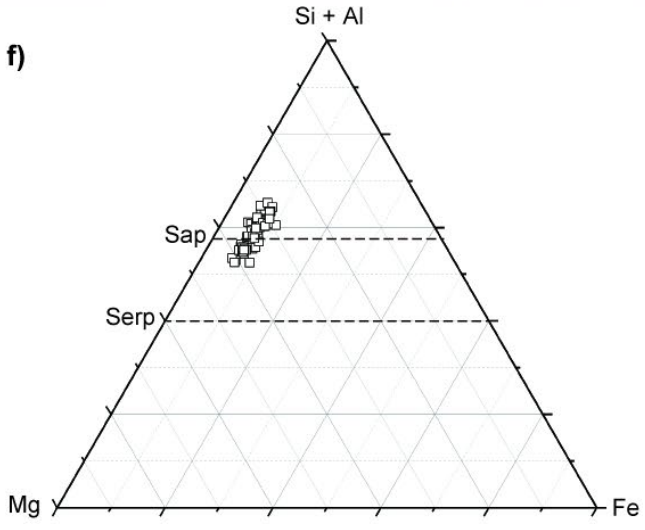
f)
Si + Al
Sap
Serp
Mg
Fe

Figure 2. TEM images and STEM-EDS analysis of a grain with a smooth surface (C0105-042_No. 24). a) High-angle annular dark-field (HAADF) image. The smooth surface coincides with a white-colored dashed line. b)–e) Elemental mapping images corresponding to the largest white-colored box in a). f) Si+Al-Mg-Fe ternary diagram (atomic ratios) of Mg-Fe phyllosilicate assemblages. The slightly Ca-rich portion at the top of the image in d) is an artifact. The area corresponds to a tungsten (W) protection layer. In this area, the intensity of the continuous X-rays is also strong along with the generation of strong characteristic X-rays from the W protection, making it appear as if calcium is apparently present. Sap: saponite, Serp: serpentine.

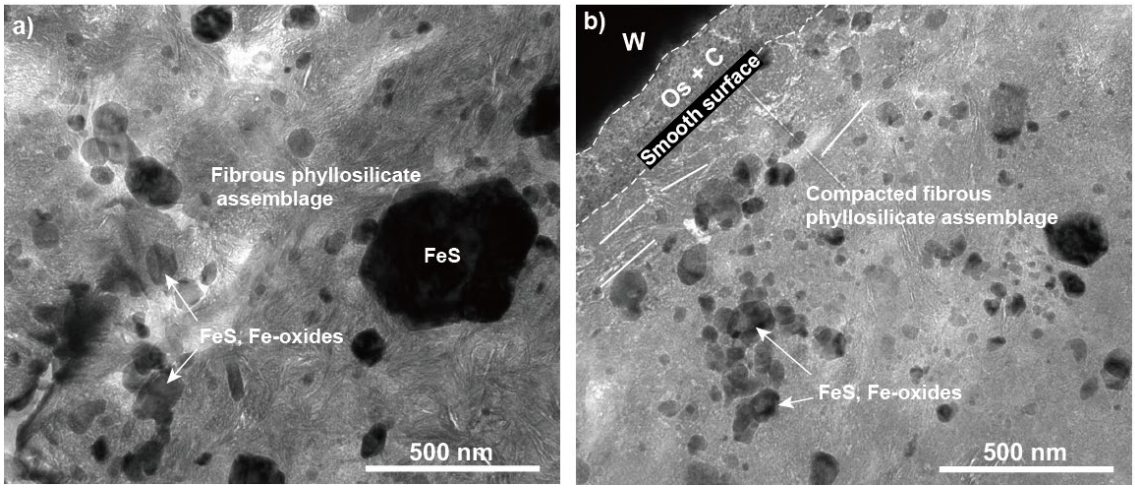

Figure 3. Bright field (BF) TEM image of matrix. a) Matrix approximately 3 μm from a smooth surface. Many interstices (bright areas in the image) are present between the fibrous Mg-Fe phyllosilicate assemblages. b) Matrix near a smooth surface. The locations of a) and b) are shown in Figure 2. FeS: iron-sulfide, Fe-oxides: iron oxides, C: carbon, Os: osmium, and W: tungsten depositions.

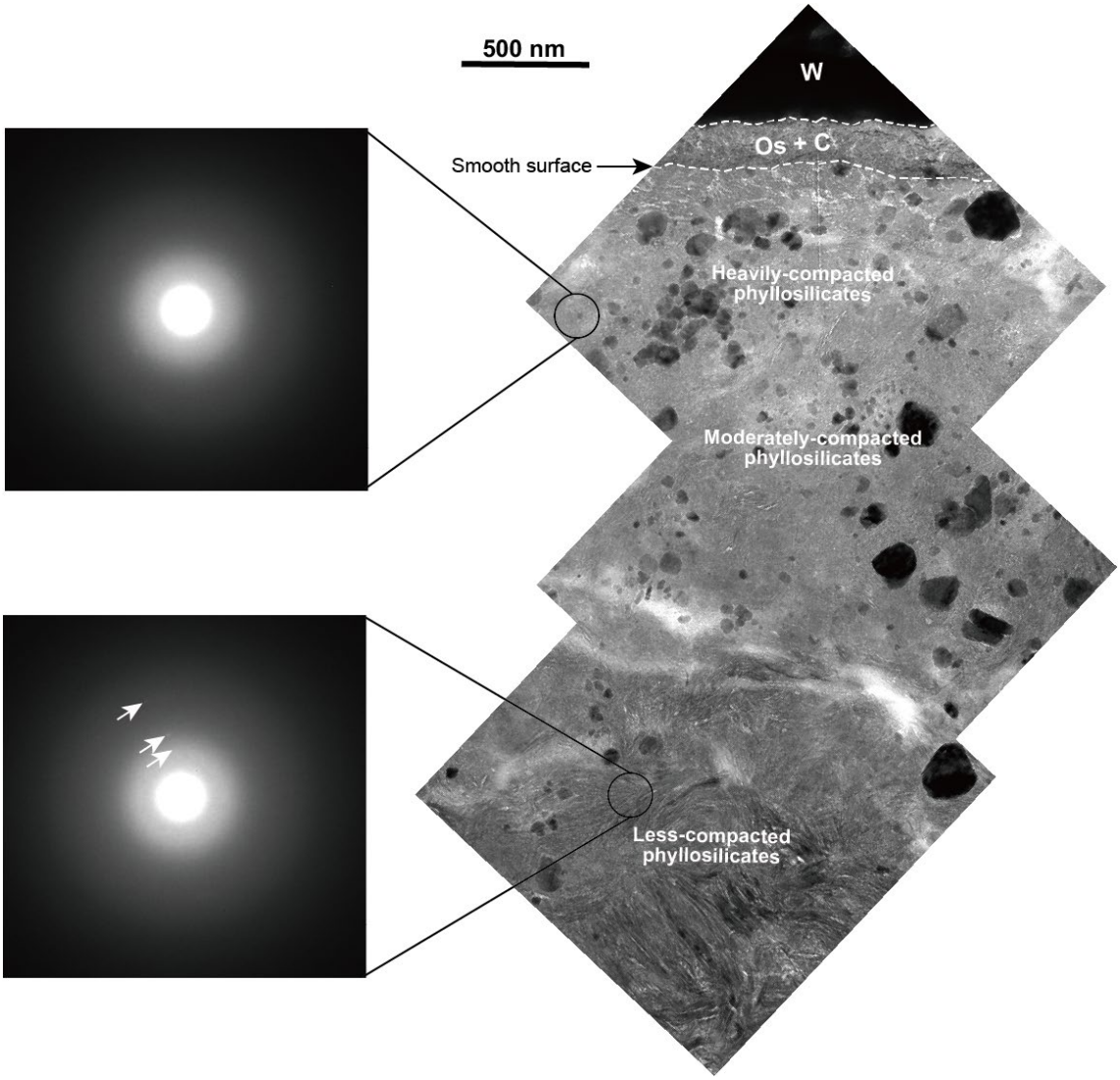

Figure 4. Mosaic BF-TEM image of a matrix beneath a smooth surface. Right insets are selected area electron diffraction (SAED) patterns corresponding to heavily-compacted (upper) and less-compacted Mg-Fe phyllosilicate assembalges (lower). Both show a halo. In the latter, the rings (white arrows) were faintly visible, but disappeared during the observation due to electron beam irradiation. C: carbon, Os: osmium, and W: tungsten depositions.

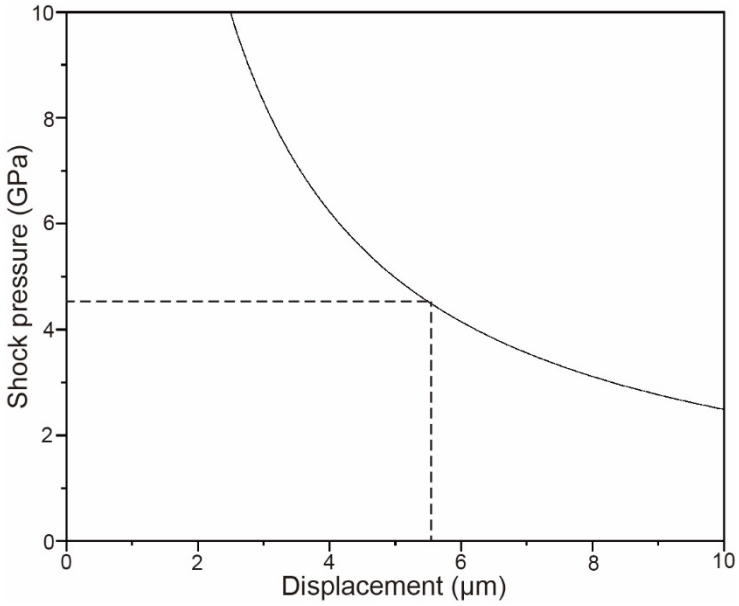

Figure 5. The calculated relationship between the displacement of microfault and shock pressure.

References

Akai J. (1992) TTT diagram of serpentine and saponite, and estimation of metamorphic heating degree of Antarctic carbonaceous chondrites. In *Sixteenth Symposium on Antarctic Meteorites*, pp. 120–135.

Anderson W. W. and Ahrens T. J. (1998) Shock wave equations of state of chondritic meteorites. In *AIP Conference Proceedings*, pp. 115–118. American Institute of Physics.

Arakawa M., Saiki T., Wada K., Ogawa K., Kadono T., Shirai K., Sawada H., Ishibashi K., Honda R., Sakatani N., Iijima Y., Okamoto C., Yano H., Takagi Y., Hayakawa M., Michel P., Jutzi M., Shimaki Y., Kimura S., Mimasu Y., Toda T., Imamura H., Nakazawa S., Hayakawa H., Sugita S., Morota T., Kameda S., Tatsumi E., Cho Y., Yoshioka K., Yokota Y., Matsuoka M., Yamada M., Kouyama T., Honda C., Tsuda Y., Watanabe S., Yoshikawa M., Tanaka S., Terui F., Kikuchi S., Yamaguchi T., Ogawa N., Ono G., Yoshikawa K., Takahashi T., Takei Y., Fujii A., Takeuchi H., Yamamoto Y., Okada T., Hirose C., Hosoda S., Mori O., Shimada T., Soldini S., Tsukizaki R., Iwata T., Ozaki M., Abe M., Namiki N., Kitazato K., Tachibana S., Ikeda H., Hirata N., Hirata N., Noguchi R., and Miura A. (2020) An artificial impact on the asteroid (162173) Ryugu formed a crater in the gravity-dominated regime. *Science* **368**, 67–71.

Ball M. C. and Taylor H. F. W. (1963) The Dehydration of Chrysotile in Air and under Hydrothermal Conditions. *Mineralogical magazine and journal of the Mineralogical Society* **33**, 467–482.

515 Baratoux D. and Reimold W. U. (2016) The current state of knowledge about shatter cones:
516 Introduction to the special issue. *Meteoritics & Planetary Science* **51**, 1389–1434.
517 Bierhaus E. B., Clark B. C., Harris J. W., Payne K. S., Dubisher R. D., Wurts D. W., Hund R. A.,
518 Kuhns R. M., Linn T. M., Wood J. L., May A. J., Dworkin J. P., Beshore E., Lauretta D.
519 S., and the O.-R. T. (2018) The OSIRIS-REx Spacecraft and the Touch-and-Go Sample
520 Acquisition Mechanism (TAGSAM). *Space Science Reviews* **214**, 107.
521 Bischoff A., Schleiting M., and Patzek M. (2018) Shock stage distribution of 2280 ordinary
522 chondrites—Can bulk chondrites with a shock stage of S6 exist as individual rocks?
523 *Meteoritics & Planetary Science* **54**, 2189–2202.
524 Bottke W. F., Moorhead A. V., Connolly Jr H. C., Hergenrother C. W., Molaro J. L., Michel P.,
525 Nolan M. C., Schwartz S. R., Vokrouhlický D., Walsh K. J., and Lauretta D. S. (2020)
526 Meteoroid Impacts as a Source of Bennu's Particle Ejection Events. *Journal of*
527 *Geophysical Research: Planets* **125**, e2019JE006282.
528 Bottke W. F., Nolan M. C., Greenberg R., and Kolvoord R. A. (1994) Velocity distributions
529 among colliding asteroids. *Icarus* **107**, 255–268.
530 Bowden F. P. and Tabor D. (2001) *The friction and lubrication of solids*. Oxford university
531 press, Oxford. pp. 424.
532 Brindley G. W. and Hayami R. (1963) Kinetics and Mechanisms of Dehydration and
533 Recrystallization of Serpentine—I. *Clays and Clay Minerals* **12**, 35–47.
534 Cattaneo A., Gualtieri A. F., and Artioli G. (2003) Kinetic study of the dehydroxylation of
535 chrysotile asbestos with temperature by in situ XRPD. *Physics and Chemistry of*
536 *Minerals* **30**, 177–183.
537 Consolmagno G. J., Britt D. T., and Macke R. J. (2008) The significance of meteorite density
538 and porosity. *Geochemistry* **68**, 1–29.
539 Doblas M., Mahecha V., Hoyos M., and Lo ´ pez-ruiz J. (1997) Slickenside and fault surface
540 kinematic indicators on active normal faults of the Alpine Betic Cordilleras, Granada,
541 southern Spain. *Journal of Structural Geology* **19**, 159–170.
542 El Goresy A., Gillet P., Miyahara M., Ohtani E., Ozawa S., Beck P., and Montagnac G. (2013)
543 Shock-induced deformation of shergottites: Shock-pressures and perturbations of
544 magmatic ages on Mars. *Geochimica et Cosmochimica Acta* **101**, 233–262.
545 Flynn G. J., Moore L. B., and Klöck W. (1999) Density and Porosity of Stone Meteorites:
546 Implications for the Density, Porosity, Cratering, and Collisional Disruption of
547 Asteroids. *Icarus* **142**, 97–105.
548 Gillet P. and El Goresy A. (2013) Shock Events in the Solar System: The Message from Minerals
549 in Terrestrial Planets and Asteroids. *Annual Review of Earth and Planetary Sciences* **41**,
550 257–285.

551 Gounelle M. and Zolensky M. E. (2001) A terrestrial origin for sulfate veins in CI1 chondrites.
552 *Meteoritics & Planetary Science* **36**, 1321–1329.
553 Grott M., Biele J., Michel P., Sugita S., Schröder S., Sakatani N., Neumann W., Kameda S.,
554 Michikami T., and Honda C. (2020) Macroporosity and Grain Density of Rubble Pile
555 Asteroid (162173) Ryugu. *Journal of Geophysical Research: Planets* **125**,
556 e2020JE006519.
557 Hamilton V. E.Simon A. A.Christensen P. R.Reuter D. C.Clark B. E.Barucci M. A.Bowles N.
558 E.Boynton W. V.Brucato J. R.Cloutis E. A.Connolly H. C.Donaldson Hanna K. L.Emery
559 J. P.Enos H. L.Fornasier S.Haberle C. W.Hanna R. D.Howell E. S.Kaplan H. H.Keller L.
560 P.Lantz C.Li J. Y.Lim L. F.McCoy T. J.Merlin F.Nolan M. C.Praet A.Rozitis B.Sandford
561 S. A.Schrader D. L.Thomas C. A.Zou X. D.Lauretta D. S.Highsmith D. E.Small
562 J.Vokrouhlický D.Bowles N. E.Brown E.Donaldson Hanna K. L.Warren T.Brunet
563 C.Chicoine R. A.Desjardins S.Gaudreau D.Haltigin T.Millington-Veloza S.Rubi
564 A.Aponte J.Gorius N.Lunsford A.Allen B.Grindlay J.Guevel D.Hoak D.Hong J.Schrader
565 D. L.Bayron J.Golubov O.Sánchez P.Stromberg J.Hirabayashi M.Hartzell C. M.Oliver
566 S.Rascon M.Harch A.Joseph J.Squyres S.Richardson D.Emery J. P.McGraw L.Ghent
567 R.Binzel R. P.Asad M. M. A.Johnson C. L.Philpott L.Susorney H. C. M.Cloutis E.
568 A.Hanna R. D.Connolly H. C.Ciceri F.Hildebrand A. R.Ibrahim E. M.Breitenfeld
569 L.Glotch T.Rogers A. D.Clark B. E.Ferrone S.Thomas C. A.Campins H.Fernandez
570 Y.Chang W.Cheuvront A.Trang D.Tachibana S.Yurimoto H.Brucato J. R.Poggiali
571 G.Pajola M.Dotto E.Mazzotta Epifani E., et al. (2019) Evidence for widespread hydrated
572 minerals on asteroid (101955) Bennu. *Nature Astronomy* **3**, 332–340.
573 Ito M.Tomioka N.Uesugi M.Yamaguchi A.Shirai N.Ohigashi T.Liu M.-C.Greenwood R.
574 C.Kimura M.Imae N.Uesugi K.Nakato A.Yogata K.Yuzawa H.Kodama Y.Tsuchiyama
575 A.Yasutake M.Findlay R.Franchi I. A.Malley J. A.McCain K. A.Matsuda N.McKeegan K.
576 D.Hirahara K.Takeuchi A.Sekimoto S.Sakurai I.Okada I.Karouji Y.Arakawa M.Fujii
577 A.Fujimoto M.Hayakawa M.Hirata N.Hirata N.Honda R.Honda C.Hosoda S.Iijima Y.-
578 i.Ikeda H.Ishiguro M.Ishihara Y.Iwata T.Kawahara K.Kikuchi S.Kitazato K.Matsumoto
579 K.Matsuoka M.Michikami T.Mimasu Y.Miura A.Mori O.Morota T.Nakazawa S.Namiki
580 N.Noda H.Noguchi R.Ogawa N.Ogawa K.Okada T.Okamoto C.Ono G.Ozaki M.Saiki
581 T.Sakatani N.Sawada H.Senshu H.Shimaki Y.Shirai K.Sugita S.Takei Y.Takeuchi
582 H.Tanaka S.Tatsumi E.Terui F.Tsukizaki R.Wada K.Yamada M.Yamada T.Yamamoto
583 Y.Yano H.Yokota Y.Yoshihara K.Yoshikawa M.Yoshikawa K.Fukai R.Furuya S.Hatakeda
584 K.Hayashi T.Hitomi Y.Kumagai K.Miyazaki A.Nishimura M.Soejima H.Iwamae
585 A.Yamamoto D.Yoshitake M.Yada T.Abe M.Usui T., et al. (2022) A pristine record of

outer Solar System materials from asteroid Ryugu's returned sample. *Nature Astronomy* **6**, 1163–1171.

Jaeger J. C., Cook N. G., and Zimmerman R. (2009) *Fundamentals of rock mechanics*. John Wiley & Sons. pp. 488.

Kanamori H., Anderson D. L., and Heaton T. H. (1998) Frictional melting during the rupture of the 1994 Bolivian earthquake. *Science* **279**, 839–842.

Kaneko S., Miyahara M., Ohtani E., Arai T., Hirao N., and Sato K. (2015) Discovery of stishovite in Apollo 15299 sample. *American Mineralogist* **100**, 1308–1311.

Kayama M., Nishido H., Sekine T., Nakazato T., Gucsik A., and Ninagawa K. (2012) Shock barometer using cathodoluminescence of alkali feldspar. *Journal of Geophysical Research: Planets* **117**, E09004.

Kieffer S. W. (1971) Shock metamorphism of the Coconino sandstone at meteor crater, Arizona. *Journal of Geophysical Research* **76**, 5449–5473.

Kikuiri M., Nakamura T., Langenhorst F., Pollok K., Mikouchi T., Yoshida H., Nakashima D., Zolensky M., Uesugi M., and Yurimoto H. (2022) Shock-Induced Deformation Recorded in the Regolith Particles from C-Type Asteroid Ryugu. In *85th Annual Meeting of The Meteoritical Society*, pp. 6199.pdf.

Kimura M., Yamaguchi A., and Miyahara M. (2017) Shock-induced thermal history of an EH3 chondrite, Asuka 10164. *Meteoritics & Planetary Science* **52**, 24–35.

Kirkpatrick J. D., Rowe C. D., White J. C., and Brodsky E. E. (2013) Silica gel formation during fault slip: Evidence from the rock record. *Geology* **41**, 1015–1018.

Lauretta D. S., Adam C. D., Allen A. J., Ballouz R.-L., Barnouin O. S., Becker K. J., Becker T., Bennett C. A., Bierhaus E. B., Bos B. J., Burns R. D., Campins H., Cho Y., Christensen P. R., Church E. C. A., Clark B. E., Connolly H. C., Daly M. G., DellaGiustina D. N., Drouet d'Aubigny C. Y., Emery J. P., Enos H. L., Kasper S. F., Garvin J. B., Getzandanner K., Golish D. R., Hamilton V. E., Hergenrother C. W., Kaplan H. H., Keller L. P., Lessac-Chenen E. J., Liounis A. J., Ma H., McCarthy L. K., Miller B. D., Moreau M. C., Morota T., Nelson D. S., Nolau J. O., Olds R., Pajola M., Pelgrift J. Y., Polit A. T., Ravine M. A., Reuter D. C., Rizk B., Rozitis B., Ryan A. J., Sahr E. M., Sakatani N., Seabrook J. A., Selznick S. H., Skeen M. A., Simon A. A., Sugita S., Walsh K. J., Westermann M. M., Wolner C. W. V., and Yumoto K. (2022) Spacecraft sample collection and subsurface excavation of asteroid (101955) Bennu. *Science* **377**, 285–291.

Macke R. J., Consolmagno G. J., and Britt D. T. (2011) Density, porosity, and magnetic susceptibility of carbonaceous chondrites. *Meteoritics & Planetary Science* **46**, 1842–1862.

Michikami T., Honda C., Miyamoto H., Hirabayashi M., Hagermann A., Irie T., Nomura K., Ernst C. M., Kawamura M., Sugimoto K., Tatsumi E., Morota T., Hirata N., Noguchi T., Cho Y., Kameda S., Kouyama T., Yokota Y., Noguchi R., Hayakawa M., Hirata N., Honda R., Matsuoka M., Sakatani N., Suzuki H., Yamada M., Yoshioka K., Sawada H., Hemmi R., Kikuchi H., Ogawa K., Watanabe S.-i., Tanaka S., Yoshikawa M., Tsuda Y., and Sugita S. (2019) Boulder size and shape distributions on asteroid Ryugu. *Icarus* **331**, 179–191.

Miyahara M., Edanaga J., Yamaguchi A., Kobayashi T., Sekine T., and Nakamura A. (2021) Chondrule Flattening by Shock Recovery Experiments on Unequilibrated Chondrites. *Journal of Geophysical Research: Planets* **126**, e2021JE006864.

Miyahara M., Yamaguchi A., Saitoh M., Fukimoto K., Sakai T., Ohfuji H., Tomioka N., Kodama Y., and Ohtani E. (2020) Systematic investigations of high-pressure polymorphs in shocked ordinary chondrites. *Meteoritics & Planetary Science* **55**, 2619–2651.

Nakamura E., Kobayashi K., Tanaka R., Kunihiro T., Kitagawa H., Potiszil C., Ota T., Sakaguchi C., Yamanaka M., Ratnayake D. M., Tripathi H., Kumar R., Avramescu M.-L., Tsuchida H., Yachi Y., Miura H., Abe M., Fukai R., Furuya S., Hatakeda K., Hayashi T., Hitomi Y., Kumagai K., Miyazaki A., Nakato A., Nishimura M., Okada T., Soejima H., Sugita S., Suzuki A., Usui T., Yada T., Yamamoto D., Yogata K., Yoshitake M., Arakawa M., Fujii A., Hayakawa M., Hirata N., Hirata N., Honda R., Honda C., Hosoda S., Iijima Y.-i., Ikeda H., Ishiguro M., Ishihara Y., Iwata T., Kawahara K., Kikuchi S., Kitazato K., Matsumoto K., Matsuoka M., Michikami T., Mimasu Y., Miura A., Morota T., Nakazawa S., Namiki N., Noda H., Noguchi R., Ogawa N., Ogawa K., Okamoto C., Ono G., Ozaki M., Saiki T., Sakatani N., Sawada H., Senshu H., Shimaki Y., Shirai K., Takei Y., Takeuchi H., Tanaka S., Tatsumi E., Terui F., Tsukizaki R., Wada K., Yamada M., Yamada T., Yamamoto Y., Yano H., Yokota Y., Yoshihara K., Yoshikawa M., Yoshikawa K., Fujimoto M., Watanabe S.-i., and Tsuda Y. (2022) On the origin and evolution of the asteroid Ryugu: A comprehensive geochemical perspective. *Proceedings of the Japan Academy, Series B* **98**, 227–282.

Nakamura T.Matsumoto M.Amano K.Enokido Y.Zolensky M. E.Mikouchi T.Genda H.Tanaka S.Zolotov M. Y.Kurosawa K.Wakita S.Hyodo R.Nagano H.Nakashima D.Takahashi Y.Fujioka Y.Kikuiri M.Kagawa E.Matsuoka M.Brearley A. J.Tsuchiyama A.Uesugi M.Matsuno J.Kimura Y.Sato M.Milliken R. E.Tatsumi E.Sugita S.Hiroi T.Kitazato K.Brownlee D.Joswiak D. J.Takahashi M.Ninomiya K.Takahashi T.Osawa T.Terada K.Brenker F. E.Tkalcec B. J.Vincze L.Brunetto R.Aleon-Toppani A.Chan Q. H. S.Roskosz M.Viennet J. C.Beck P.Alp E. E.Michikami T.Nagaashi Y.Tsuji T.Ino Y.Martinez J.Han J.Dolocan A.Bodnar R. J.Tanaka M.Yoshida H.Sugiyama K.King A.

J.Fukushi K.Suga H.Yamashita S.Kawai T.Inoue K.Nakato A.Noguchi T.Vilas F.Hendrix A. R.Jaramillo-Correa C.Domingue D. L.Dominguez G.Gainsforth Z.Engrand C.Duprat J.Russell S. S.Bonato E.Ma C.Kawamoto T.Wada T.Watanabe S.Endo R.Enju S.Riu L.Rubino S.Tack P.Takeshita S.Takeichi Y.Takeuchi A.Takigawa A.Takir D.Tanigaki T.Taniguchi A.Tsukamoto K.Yagi T.Yamada S.Yamamoto K.Yamashita Y.Yasutake M.Uesugi K.Umegaki I., et al. (2023) Formation and evolution of carbonaceous asteroid Ryugu: Direct evidence from returned samples. *Science* **379**, eabn8671.

Nakamura T., Tomeoka K., Takaoka N., Sekine T., and Takeda H. (2000) Impact-induced textural changes of CV carbonaceous chondrites: Experimental reproduction. *Icarus* **146**, 289–300.

Noguchi T.Matsumoto T.Miyake A.Igami Y.Haruta M.Saito H.Hata S.Seto Y.Miyahara M.Tomioka N.Ishii H. A.Bradley J. P.Ohtaki K. K.Dobrică E.Leroux H.Le Guillou C.Jacob D.de la Peña F.Laforet S.Marinova M.Langenhorst F.Harries D.Beck P.Phan T. H. V.Rebois R.Abreu N. M.Gray J.Zega T.Zanetta P.-M.Thompson M. S.Stroud R.Burgess K.Cymes B. A.Bridges J. C.Hicks L.Lee M. R.Daly L.Bland P. A.Zolensky M. E.Frank D. R.Martinez J.Tsuchiyama A.Yasutake M.Matsuno J.Okumura S.Mitsukawa I.Uesugi K.Uesugi M.Takeuchi A.Sun M.Enju S.Takigawa A.Michikami T.Nakamura T.Matsumoto M.Nakauchi Y.Abe M.Arakawa M.Fujii A.Hayakawa M.Hirata N.Hirata N.Honda R.Honda C.Hosoda S.Iijima Y.-i.Ikeda H.Ishiguro M.Ishihara Y.Iwata T.Kawahara K.Kikuchi S.Kitazato K.Matsumoto K.Matsuoka M.Mimasu Y.Miura A.Morota T.Nakazawa S.Namiki N.Noda H.Noguchi R.Ogawa N.Ogawa K.Okada T.Okamoto C.Ono G.Ozaki M.Saiki T.Sakatani N.Sawada H.Senshu H.Shimaki Y.Shirai K.Sugita S.Takei Y.Takeuchi H.Tanaka S.Tatsumi E.Terui F., et al. (2023) A dehydrated space-weathered skin cloaking the hydrated interior of Ryugu. *Nature Astronomy* **7**, 170–181.

Ogawa K., Sakatani N., Kadono T., Arakawa M., Honda R., Wada K., Shirai K., Shimaki Y., Ishibashi K., Yokota Y., Saiki T., Imamura H., Tsuda Y., Nakazawa S., Takagi Y., Hayakawa M., Yano H., Okamoto C., Iijima Y., Morota T., Kameda S., Tatsumi E., Cho Y., Yoshioka K., Sawada H., Matsuoka M., Yamada M., Kouyama T., Suzuki H., Honda C., and Sugita S. (2022) Particle size distributions inside and around the artificial crater produced by the Hayabusa2 impact experiment on Ryugu. *Earth, Planets and Space* **74**, 153.

Ohtani E., Kimura Y., Kimura M., Takata T., Kondo T., and Kubo T. (2004) Formation of high-pressure minerals in shocked L6 chondrite Yamato 791384: constraints on shock conditions and parent body size. *Earth and Planetary Science Letters* **227**, 505–515.

692 Okazaki R.Marty B.Busemann H.Hashizume K.Gilmour J. D.Meshik A.Yada T.Kitajima
693 F.Broadley M. W.Byrne D.Füri E.Riebe M. E. I.Krietsch D.Maden C.Ishida A.Clay
694 P.Crowther S. A.Fawcett L.Lawton T.Pravdivtseva O.Miura Y. N.Park J.Bajo K.-
695 i.Takano Y.Yamada K.Kawagucci S.Matsui Y.Yamamoto M.Righter K.Sakai S.Iwata
696 N.Shirai N.Sekimoto S.Inagaki M.Ebihara M.Yokochi R.Nishiizumi K.Nagao K.Lee J.
697 I.Kano A.Caffee M. W.Uemura R.Nakamura T.Naraoka H.Noguchi T.Yabuta
698 H.Yurimoto H.Tachibana S.Sawada H.Sakamoto K.Abe M.Arakawa M.Fujii A.Hayakawa
699 M.Hirata N.Hirata N.Honda R.Honda C.Hosoda S.Iijima Y.-i.Ikeda H.Ishiguro
700 M.Ishihara Y.Iwata T.Kawahara K.Kikuchi S.Kitazato K.Matsumoto K.Matsuoka
701 M.Michikami T.Mimasu Y.Miura A.Morota T.Nakazawa S.Namiki N.Noda H.Noguchi
702 R.Ogawa N.Ogawa K.Okada T.Okamoto C.Ono G.Ozaki M.Saiki T.Sakatani N.Senshu
703 H.Shimaki Y.Shirai K.Sugita S.Takei Y.Takeuchi H.Tanaka S.Tatsumi E.Terui
704 F.Tsukizaki R.Wada K.Yamada M.Yamada T.Yamamoto Y.Yano H., et al. (2023) Noble
705 gases and nitrogen in samples of asteroid Ryugu record its volatile sources and recent
706 surface evolution. *Science* **379**, eabo0431.
707 Otsuki M. and Matsukawa H. (2013) Systematic Breakdown of Amontons' Law of Friction for an
708 Elastic Object Locally Obeying Amontons' Law. *Scientific Reports* **3**, 1586.
709 Power W. L. and Tullis T. E. (1989) The relationship between slickenside surfaces in fine-
710 grained quartz and the seismic cycle. *Journal of Structural Geology* **11**, 879–893.
711 Richardson S. M. (1978) Vein formation in the C1 carbonaceous chondrites. *Meteoritics* **13**,
712 141–159.
713 Rinaldi G., Della Corte V., Fulle M., Capaccioni F., Rotundi A., Ivanovski S. L., Bockelée-
714 Morvan D., Filacchione G., D'Aversa E., Capria M. T., Tozzi G. P., Erard S., Leyrat C.,
715 Palomba E., Longobardo A., Ciarniello M., Taylor F., Mottola S., and Salatti M. (2017)
716 Cometary coma dust size distribution from in situ IR spectra. *Monthly Notices of the*
717 *Royal Astronomical Society* **469**, S598–S605.
718 Sagy A. and Brodsky E. E. (2009) Geometric and rheological asperities in an exposed fault zone.
719 *Journal of Geophysical Research: Solid Earth* **114**, B02301.
720 Scott E. R. D., Keil K., and Stöffler D. (1992) Shock metamorphism of carbonaceous chondrites.
721 *Geochimica et Cosmochimica Acta* **56**, 4281–4293.
722 Sharp T. G. and DeCarli P. S. (2006) Shock effects in meteorites. In *Meteorites and the early*
723 *solar system II* (ed. H. Y. M. Dante S. Lauretta, Jr.), pp. 653–677. Univ of Arizona
724 Press, Tucson.
725 Stöffler D., Hamann C., and Metzler K. (2018) Shock metamorphism of planetary silicate rocks
726 and sediments: Proposal for an updated classification system. *Meteoritics & Planetary*
727 *Science* **53**, 5–49.

Sugita S.Honda R.Morota T.Kameda S.Sawada H.Tatsumi E.Yamada M.Honda C.Yokota Y.Kouyama T.Sakatani N.Ogawa K.Suzuki H.Okada T.Namiki N.Tanaka S.Iijima Y.Yoshioka K.Hayakawa M.Cho Y.Matsuoka M.Hirata N.Hirata N.Miyamoto H.Domingue D.Hirabayashi M.Nakamura T.Hiroi T.Michikami T.Michel P.Ballouz R.-L.Barnouin O. S.Ernst C. M.Schröder S. E.Kikuchi H.Hemmi R.Komatsu G.Fukuhara T.Taguchi M.Arai T.Senshu H.Demura H.Ogawa Y.Shimaki Y.Sekiguchi T.Müller T. G.Hagermann A.Mizuno T.Noda H.Matsumoto K.Yamada R.Ishihara Y.Ikeda H.Araki H.Yamamoto K.Abe S.Yoshida F.Higuchi A.Sasaki S.Oshigami S.Tsuruta S.Asari K.Tazawa S.Shizugami M.Kimura J.Otsubo T.Yabuta H.Hasegawa S.Ishiguro M.Tachibana S.Palmer E.Gaskell R.Le Corre L.Jaumann R.Otto K.Schmitz N.Abell P. A.Barucci M. A.Zolensky M. E.Vilas F.Thuillet F.Sugimoto C.Takaki N.Suzuki Y.Kamiyoshihara H.Okada M.Nagata K.Fujimoto M.Yoshikawa M.Yamamoto Y.Shirai K.Noguchi R.Ogawa N.Terui F.Kikuchi S.Yamaguchi T.Oki Y.Takao Y.Takeuchi H.Ono G., et al. (2019) The geomorphology, color, and thermal properties of Ryugu: Implications for parent-body processes. *Science* **364**, eaaw0422.

Tachibana S.Sawada H.Okazaki R.Takano Y.Sakamoto K.Miura Y. N.Okamoto C.Yano H.Yamanouchi S.Michel P.Zhang Y.Schwartz S.Thuillet F.Yurimoto H.Nakamura T.Noguchi T.Yabuta H.Naraoka H.Tsuchiyama A.Imae N.Kurosawa K.Nakamura A. M.Ogawa K.Sugita S.Morota T.Honda R.Kameda S.Tatsumi E.Cho Y.Yoshioka K.Yokota Y.Hayakawa M.Matsuoka M.Sakatani N.Yamada M.Kouyama T.Suzuki H.Honda C.Yoshimitsu T.Kubota T.Demura H.Yada T.Nishimura M.Yogata K.Nakato A.Yoshitake M.Suzuki A. I.Furuya S.Hatakeda K.Miyazaki A.Kumagai K.Okada T.Abe M.Usui T.Ireland T. R.Fujimoto M.Yamada T.Arakawa M.Connolly H. C.Fujii A.Hasegawa S.Hirata N.Hirata N.Hirose C.Hosoda S.Iijima Y.Ikeda H.Ishiguro M.Ishihara Y.Iwata T.Kikuchi S.Kitazato K.Lauretta D. S.Libourel G.Marty B.Matsumoto K.Michikami T.Mimasu Y.Miura A.Mori O.Nakamura-Messenger K.Namiki N.Nguyen A. N.Nittler L. R.Noda H.Noguchi R.Ogawa N.Ono G.Ozaki M.Senshu H.Shimada T.Shimaki Y.Shirai K.Soldini S.Takahashi T.Takei Y.Takeuchi H.Tsukizaki R.Wada K.Yamamoto Y., et al. (2022) Pebbles and sand on asteroid (162173) Ryugu: In situ observation and particles returned to Earth. *Science* **375**, 1011–1016.

Tomeoka K., Kiriyama K., Nakamura K., Yamahana Y., and Sekine T. (2003) Interplanetary dust from the explosive dispersal of hydrated asteroids by impacts. *Nature* **423**, 60–62.

Tomeoka K., Ohnishi I., and Nakamura N. (2001) Silicate darkening in the Kobe CK chondrite: Evidence for shock metamorphism at high temperature. *Meteoritics & Planetary Science* **36**, 1535–1545.

764 Tomeoka K., Yamahana Y., and Sekine T. (1999) Experimental shock metamorphism of the
765 Murchison CM carbonaceous chondrite. *Geochimica et Cosmochimica Acta* **63**, 3683–
766 3703.
767 Tomioka N. and Miyahara M. (2017) High - pressure minerals in shocked meteorites.
768 *Meteoritics & Planetary Science* **52**, 2017–2039.
769 Tomioka N., Tomeoka K., Nakamura-Messenger K., and Sekine T. (2007) Heating effects of the
770 matrix of experimentally shocked Murchison CM chondrite: Comparison with
771 micrometeorites. *Meteoritics & Planetary Science* **42**, 19–30.
772 Tomioka N., Yamaguchi A., Ito M., Uesugi M., Imae N., Shirai N., Ohigashi T., Kimura M., Liu
773 M.-C., Greenwood R. C., Uesugi K., Nakato A., Yogata K., Yuzawa H., Kodama Y.,
774 Hirahara K., Sakurai I., Okada I., Karouji Y., Okazaki K., Kurosawa K., Noguchi T.,
775 Miyake A., Miyahara M., Seto Y., Matsumoto T., Igami Y., Nakazawa S., Okada T., Saiki
776 T., Tanaka S., Terui F., Yoshikawa M., Miyazaki A., Nishimura M., Yada T., Abe M.,
777 Usui T., Watanabe S.-i., and Tsuda Y. (2023) A history of mild shocks experienced by
778 the regolith particles on hydrated asteroid Ryugu. *Nature Astronomy*,
779 doi.org/10.1038/s41550-023-01947-5.
780 Tsuchiyama A., Mashio E., Imai Y., Noguchi T., Miura Y. N., and Yano H. (2008) Strength
781 measurements of carbonaceous chondrites and cosmic dust analogs using micro
782 compression testing machine. In *Japan Geosciences Union Meeting, Abstracts of Papers*,
783 pp. P168-002.
784 Watanabe S., Hirabayashi M., Hirata N., Hirata N., Noguchi R., Shimaki Y., Ikeda H., Tatsumi
785 E., Yoshikawa M., Kikuchi S., Yabuta H., Nakamura T., Tachibana S., Ishihara Y.,
786 Morota T., Kitazato K., Sakatani N., Matsumoto K., Wada K., Senshu H., Honda C.,
787 Michikami T., Takeuchi H., Kouyama T., Honda R., Kameda S., Fuse T., Miyamoto H.,
788 Komatsu G., Sugita S., Okada T., Namiki N., Arakawa M., Ishiguro M., Abe M., Gaskell
789 R., Palmer E., Barnouin O. S., Michel P., French A. S., McMahon J. W., Scheeres D. J.,
790 Abell P. A., Yamamoto Y., Tanaka S., Shirai K., Matsuoka M., Yamada M., Yokota Y.,
791 Suzuki H., Yoshioka K., Cho Y., Tanaka S., Nishikawa N., Sugiyama T., Kikuchi H.,
792 Hemmi R., Yamaguchi T., Ogawa N., Ono G., Mimasu Y., Yoshikawa K., Takahashi T.,
793 Takei Y., Fujii A., Hirose C., Iwata T., Hayakawa M., Hosoda S., Mori O., Sawada H.,
794 Shimada T., Soldini S., Yano H., Tsukizaki R., Ozaki M., Iijima Y., Ogawa K., Fujimoto
795 M., Ho T.-M., Moussi A., Jaumann R., Bibring J.-P., Krause C., Terui F., Saiki T.,
796 Nakazawa S., and Tsuda Y. (2019) Hayabusa2 arrives at the carbonaceous asteroid
797 162173 Ryugu-A spinning top-shaped rubble pile. *Science* **364**, 268–272.
798 Weber J. N. and Greer R. T. (1965) Dehydration of serpentine: heat of reaction and reaction
799 kinetics at P_{H2O}=1 ATM. *American Mineralogist* **50**, 450–464.

Weisberg M. K., McCoy T. J., and Krot A. N. (2006) Systematics and evaluation of meteorite classification. In *Meteorites and the early solar system II* (eds. D. S. Lauretta and H. Y. McSween Jr), pp. 19–52. The University of Arizona Press, Arizona.

Yokoyama T.Nagashima K.Nakai I.Young E. D.Abe Y.Aléon J.Alexander C. M. O. D.Amari S.Amelin Y.Bajo K.-i.Bizzarro M.Bouvier A.Carlson R. W.Chaussidon M.Choi B.-G.Dauphas N.Davis A. M.Di Rocco T.Fujiya W.Fukai R.Gautam I.Haba M. K.Hibiya Y.Hidaka H.Homma H.Hoppe P.Huss G. R.Ichida K.Iizuka T.Ireland T. R.Ishikawa A.Ito M.Itoh S.Kawasaki N.Kita N. T.Kitajima K.Kleine T.Komatani S.Krot A. N.Liu M.-C.Masuda Y.McKeegan K. D.Morita M.Motomura K.Moynier F.Nguyen A.Nittler L.Onose M.Pack A.Park C.Piani L.Qin L.Russell S. S.Sakamoto N.Schönbächler M.Tafla L.Tang H.Terada K.Terada Y.Usui T.Wada S.Wadhwa M.Walker R. J.Yamashita K.Yin Q.-Z.Yoneda S.Yui H.Zhang A.-C.Connolly H. C.Lauretta D. S.Nakamura T.Naraoka H.Noguchi T.Okazaki R.Sakamoto K.Yabuta H.Abe M.Arakawa M.Fujii A.Hayakawa M.Hirata N.Hirata N.Honda R.Honda C.Hosoda S.Iijima Y.-i.Ikeda H.Ishiguro M.Ishihara Y.Iwata T.Kawahara K.Kikuchi S.Kitazato K.Matsumoto K.Matsuoka M.Michikami T.Mimasu Y.Miura A.Morota T.Nakazawa S., et al. (2023) Samples returned from the asteroid Ryugu are similar to Ivuna-type carbonaceous meteorites. *Science* **379**, eabn7850.

Zolensky M., Martinez J., Sitzman S., Mikouchi T., Hagiya K., Ohsumi K., Komatsu M., Nakamura T., Takenouchi A., Ono H., Hasegawa H., Higashi K., Terada Y., Yagi N., Takata M., Ozawa H., Taki Y., Yamatsuta Y., Hirata A., Kurokawa A., and Yamaguchi S. (2022a) Measuring the shock stage of Itokawa and asteroid regolith grains by electron backscattered diffraction, optical petrography, and synchrotron X-ray diffraction. *Meteoritics & Planetary Science* **57**, 1060–1078.

Zolensky M., Mikouchi T., Hagiya K., Ohsumi K., Komatsu M., Cheng A., and Le L. (2022b) Evidence for impact shock and regolith transportation on CM, CI, and CV chondrite parent asteroids. *Meteoritics & Planetary Science* **57**, 1902–1919.